The Sexual Segment of *Hemidactylus turcicus* and the Evolution of Sexual Segment Location in Squamata

Justin L. Rheubert,[1]* Christopher M. Murray,[1] Dustin S. Siegel,[1,2] Johnathan Babin,[1] and David M. Sever[1]

[1]*Department of Biological Sciences, Southeastern Louisiana University, SLU 10736, Hammond, Louisiana 70402*
[2]*Department of Biological Sciences, Saint Louis University, St. Louis, Missouri 63103*

ABSTRACT The kidneys of the Mediterranean Gecko, *Hemidactylus turcicus* (Gekkonidae), were investigated using light and electron microscopy with the primary focus placed on morphology of the sexual segment of the kidney. The nephrons of male *H. turcicus* are composed of five distinct regions: 1) a renal corpuscle and glomerulus, 2) a proximal convoluted tubule, 3) an intermediate segment, 4) a distal convoluted tubule, and 5) the sexual segment of the kidney/collecting duct. Female *H. turcicus* is similar but lack a sexual segment of the kidney. The sexual segment of the kidney is hypertrophied during the months of March through August, which corroborates previous reports of reproductive activity. During inactive months, the sexual segment of the kidney is nondiscernable from the collecting ducts. The sexual segment consists of tall columnar epithelial cells with basally positioned nuclei. Perinuclear Golgi complexes and rough endoplasmic reticulum are present. Secretory granules, which fill the apices of the epithelial cells, are electron dense and released into the lumen by a merocrine secretory process. Narrow intercellular canaliculi separate each epithelial cell and are sealed by tight junctions at the luminal aspect. Basally, leukoctyes are observed within the intercellular canaliculi and outside the basal lamina. Mast cells can be found just outside the basal lamina in close association with renal capillaries. The sexual segment of the kidney of *H. turcicus* is similar to that of three unrelated lizards for which ultrastructure was investigated with secretion mode being the major difference Also, *H. turcicus* is similar to most other lizards in that complete regression occurs during reproductive inactivity, but differs in this trait from the skink, *Scincella lateralis*, and most snakes which display a hypertrophied sexual segment of the kidney throughout the entire year. Although some unique similarities appear during the optimization, no direct patterns or directions are observed, and only the molecular based phylogeny resolves the ancestral condition of the Squamata as the sexual segment of the kidney being observed in the distal convoluted tubule, collecting duct, and ureter. J. Morphol. 272:802–813, 2011.

KEY WORDS: reproduction; kidney; sexual segment; histology; gecko

INTRODUCTION

The sexual segment of the kidney (SSK) was first described as a hypertrophied region of the kidney ducts by Gampert (1866) in the grass snake, *Natrix natrix,* and termed the "segment sexuel" by Regaud and Policard (1903), who noted the SSK occurred only in male snakes. Subsequently, the SSK has been found in the kidney ducts of all male snakes and lizards (Squamata) that have been examined and is considered a secondary sexual characteristic (reviews by Saint Girons, 1972; Fox, 1977; Aldridge et al., in press). Research has been conducted investigating the morphology and physiology of the sexual segment in many squamates, but only nine studies have investigated ultrastructural characteristics of the SSK, five on snakes (Kühnnel and Krisch, 1974; Sever et al., 2002; Krohmer, 2004; Sever et al., 2008; Siegel et al., 2009), and four on lizards (Furieri and Lanzavecchia, 1959; Del Conte and Tamayo, 1973; Gabri 1983; Sever and Hopkins, 2005).

Previous studies regarding the sexual segment vary in depth of coverage. For lizards, Furieri and Lanzavecchia (1959) were concerned only with the effects of castration on the ergastoplasm (endoplasmic reticulum conditions) of the sexual segment of Italian wall lizards, *Lacerta sicula* (Lacertidae). Del Conte and Tamayo (1973) compared the sexual segment of males of rainbow whiptails, *Cnemidophorus lemniscatus* (Teiidae), with a homologous area that undergoes some differentiation in females. Gabri (1983) examined captives of Balkan wall lizards, *Podacris taurica* (Lacertidae), kept under temperatures mimicking natural

Additional Supporting Information may be found in the online version of this article.

Contract grant sponsor: National Science Foundation; Contract grant number: DEB-0809831.

*Correspondence to: Justin L. Rheubert, Department of Biological Sciences, Southeastern Louisiana University, SLU 10736, Hammond, LA 70402. E-mail: Justin.Rheubert@selu.edu

Received 27 October 2010; Revised 18 November 2010; Accepted 29 November 2010

Published online 28 April 2011 in Wiley Online Library (wileyonlinelibrary.com)
DOI: 10.1002/jmor.10949

conditions but a complete annual cycle was not examined. Sever and Hopkins (2005) studied seasonal variation at the light- and electron-microscopy level of the SSK in the ground skink, *Scincella lateralis* (Scincidae). They reported data from wild-caught lizards collected throughout the entire year and found that, like most snakes (Aldridge et al., in press), the SSK of *S. lateralis* is discernible from other nephridic tubules during the inactive season, which differs from that of other lizards (Sever et al., 2002). They also provided ultrastructural observations on corresponding areas of the female urinary ducts, and, like *C. lemniscatus*, a hypertrophid region similar to that of the male was found in females.

Sever et al. (2002) proposed that the SSK is a synapomorphy for squamates and possibly lepidosaurs (Sphenodon + Squamata), as a SSK may also be present in tuataras, *Sphenodon punctatus* (Gabe and Saint Girons, 1964). However, a secretory region of the kidney is also developed in stickleback fish (Courrier, 1922) and in at least three families of salamanders (Siegel et al., 2010). However, sexual kidney structures in these other vertebrate taxa do not appear to be homologous with those found in the lepidosaurian reptiles (Siegel and Aldridge, personal communication).

The function of the SSK has yet to be fully elucidated, but the SSK has been hypothesized to activate and sustain sperm (Bishop, 1959; Cuellar, 1966), form copulatory plugs after insemination (Devine, 1975), provide courtship pheromones (Volsøe, 1944), and/or provide other functions associated with seminal fluid (Prasad and Reddy, 1972). Seasonal variation in the SSK has shown strong correlation with spermatogenic activity, mating, and increased androgen levels (Bishop, 1959; Pandha and Thapliyal, 1964; Misra et al., 1965; Prasad and Sanyal, 1969; Krohmer, 1986).

Earlier research found that variation exists in the location of the SSK between different species of squamates. In most snakes, the SSK includes portions of the distal convoluted tubule (Fox, 1977), and in the scolecophidia, the SSK is limited to the collecting duct portions of the kidney (Fox, 1965). However, recent studies have shown that the SSK in lizards is highly variable (Saint Girons, 1972; Sever and Hopkins, 2005).

Although the SSK of geckos has been examined with light microscopy (Misra et al., 1965; Sanyal and Prasad, 1966; Saint Girons, 1972), no ultrastructural studies exist. In southern Louisiana Mediterranean geckos, *Hemidactylus turcicus,* are spermatogenically active during the months of October through August. Spermiation begins in December and is most intense February through July (Rheubert et al., 2009). Here, we describe the seasonal ultrastructure of the SSK in a gecko, *H. turcicus*. We then compare these data with those of other ultrastructural studies on squamate SSKs. To better understand the evolution of the SSK in a broad context, we then optimize SSK location on alternate squamate phylogenetic hypotheses.

MATERIALS AND METHODS

Tissue Collection

Adult male *H. turcicus* were collected from southeast Louisiana from March 2007–March 2008 with the exception of December, and a reproductively active female from April 2007 was examined. Geckos were euthanized within 48 h of capture using a 0.2–0.5 ml intraperitoneal injection of sodium pentabarbitol as approved by the Animal Care and Use Committee of Southeastern Louisiana University. Snout-vent lengths were measured to the nearest 0.1 mm using calipers. The urogenital systems were removed through gross dissection with the right side fixed in neutral buffered formalin for light microscopy and the left side fixed in Trump's solution for electron microscopy. Carcasses of all specimens were deposited in the Southeastern Louisiana University Vertebrate Museum.

Light Microscopy

After fixation, tissues were rinsed with deionized water, dehydrated through a graded series of ethanol solutions (70%, 80%, 95% × 2, 100% × 2), cleared in two changes of toluene, and placed in melted paraffin for 24 h under vacuum. Tissues were then embedded in paraffin blocks and allowed to cure overnight. Paraffin sections were cut at 10 μm with a RMC rotary microtome (RMC Instruments, Tucson, AZ) and placed on albuminized slides. Alternate slides were stained with hematoxylin and eosin (general histological examination), bromphenol blue (protein concentrations), and periodic acid and Schiff reagent (PAS, neutral carbohydrates) counterstained with alcian blue 8GX at pH 2.5 (carboxylated glycosaminoglycans). Slides were viewed using a Leica DM2000 compound microscope and photographs were taken using a Leica DF420 digital camera (Leica Microsystems, Wetzlar, Germany). Composite micrographs were constructed using Adobe Photoshop 7.0 (Adobe Systems, San Jose, CA).

Electron Microscopy

Tissues for transmission electron microscopy were rinsed in deionized water, postfixed in 2% osmium tetroxide, dehydrated through a graded series of ethanol solutions (0%, 85%, 95% × 2, 100% × 2), cleared in propylene oxide, and embedded in epoxy resin (Embed 812, Electron Microscopy Sciences, Hatfield, PA). Plastic sections were cut using a Reichert ultramicrotome (Reichert Microscope Services, Depew, NY) and DiATOME (Biel, Switzerland) diamond knives at 1 μm and 70 nm. Toluidine blue was used to stain 1 μm thick sections to highlight areas for electron microscopy examination. Sections 70 nm in thickness were placed on uncoated 200 mesh copper grids (Electron Microscopy Sciences, Hatfield, PA) and stained with uranyl acetate and lead citrate. Grids were viewed using a JEOL 100 transmission electron microscope (JEOL, Tokyo, Japan) and photographed using a L3C CCD attached digital camera (Scientific Instruments and Applications, Duluth, GA). Specimens for scanning electron microscopy were dehydrated using a series of graded ethanol solutions, critical point dried with a Denton DCP-1, and sputter coated with gold palladium using a Denton Desk IV (Denton Vacuum, Moorestown, NJ). Specimens were viewed and photographed using a Phillips XL20 scanning electron microscope. Composite micrographs were again constructed using Adobe Photoshop 7.0 (Adobe Systems, San Jose, CA).

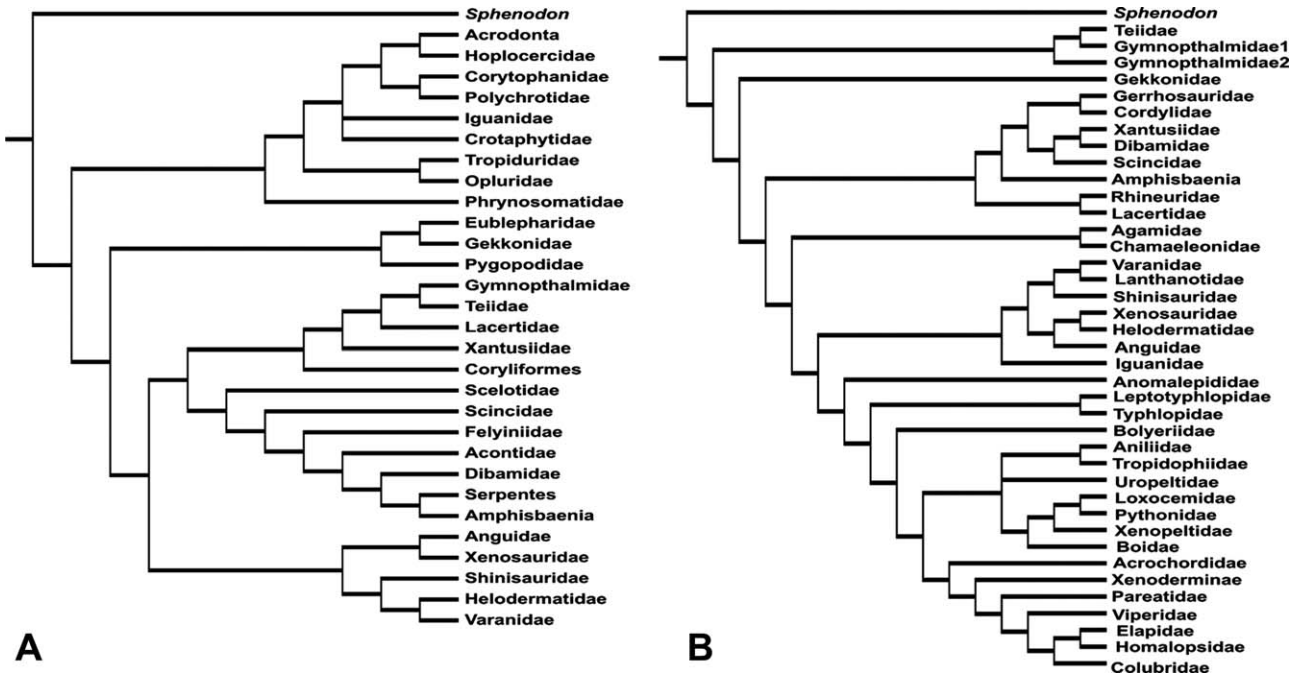

Fig. 1. Phylogenetic hypotheses used for character mapping in assessing evolutionary trends. **A.** Morphological phylogeny provided by Conrad (2008). **B.** Molecular phylogeny provided by Eckstut et al. (2009b).

Phylogenetic Analysis

Character optimization was performed using MacClade (version 4.08; Maddison and Maddison 2005) under a most parsimonious reconstruction framework. All historical data were acquired from previously published light micrographs by a single author (J.L.R.). Taxa sampled, character states, and references used are shown in the Supporting Information. The character states of taxa were elevated and assigned to that member's family level unless multiple taxa within a family presented differing character states. For instance, the character state of *Varanus niloticus* (obtained from Saint Girons 1972) was assigned to Varanidae, because the necessary reproductive morphology of all members of each family has not been described in the literature. We identified five distinct regions of the SSK in squamates: limited to collecting duct (Character 0); limited to the distal convoluted tubule, collecting duct, and ureter (Character 1); limited to collecting duct and ureter (Character 2); limited to distal convoluted tubule (Character 3); and limited to intermediate segment (Character 4).

Character states were optimized onto the squamate phylogeny of Conrad (2008) (Fig. 1A) and Eckstut et al. (2009b) (Fig. 1B) separately. The Conrad (2008) phylogenetic hypothesis of Squamata provides an extensive morphological tree reconstructed with the use osteological data. Eckstut et al. (2009b) provide a squamate level phylogeny using the nuclear encoded C-mos gene. All attempts were made to synonymize the taxonomy between the two phylogenies. The Conrad (2008) clade comprised of Pygopodidae, Eublepharidae, and Gekkonidae was collapsed to strictly Gekkonidae to match Eckstut et al. (2009b) taxonomy. The Pygopodidae character state for RSS location is unknown, whereas the Eublepharidae and Gekkonidae share character state 0. Character state 0 is applied to the collapsed Gekkonidae clade. In the Eckstut et al. (2009b) phylogeny, the Cordylidae and Gerrhosauridae clade was collapsed into a single Cordyliformes clade and the Chameleonidae and Agamidae clade was collapsed into a single Acrodonta clade. Differences in taxonomy on the resulting character mapping trees are a result of incrongruenices between the two alternate hypotheses. Conrad (2008) elevates subfamilial clades (Polychrotidae, Phrynosomatidae, Opluridae, and Corytophanidae) to family level because the hypothesized family Iguanidae is rendered paraphyletic by Acrodonta and Hoplocercidae in his resulting phylogeny. Eckstut et al. (2009b) recover a monophyletic Iguanidae and retains sub familial levels. Descriptive statistics were not incorporated into this analysis, because taxon sampling is low and gaps in the data exist (Helodermatidae, Xenosauridae, etc.).

RESULTS

Gross and Light Microscopy

The kidneys of *H. turcicus* are retropleuroperitoneal and lie along the dorsal wall lateral to the spinal column. The ductus deferens runs ventral to the kidney within the hilus groove but external to the collagen sheath surrounding the kidney. The nephridian tubules consist of five main regions (Fig. 2): a) a renal corpuscle and glomerulus, b) a proximal convoluted tubule, c) an intermediate segment, d) a distal convoluted tubule, and e) the SSK. The histology of the nephron is described below from a reproductively active male *H. turcicus*.

The small renal corpuscle possesses a squamous parietal and visceral epithelium (Fig. 2A) that stains positively with alcian blue (Fig. 3B). The visceral epithelium is in direct contact with the capillaries of the glomerulus (Fig. 2A). The simple low columnar epithelium of the proximal convoluted tubule (Fig. 2B) is continuous with the epithelium of the renal corpuscle. The epithelial cells of this region are filled with dark staining cyto-

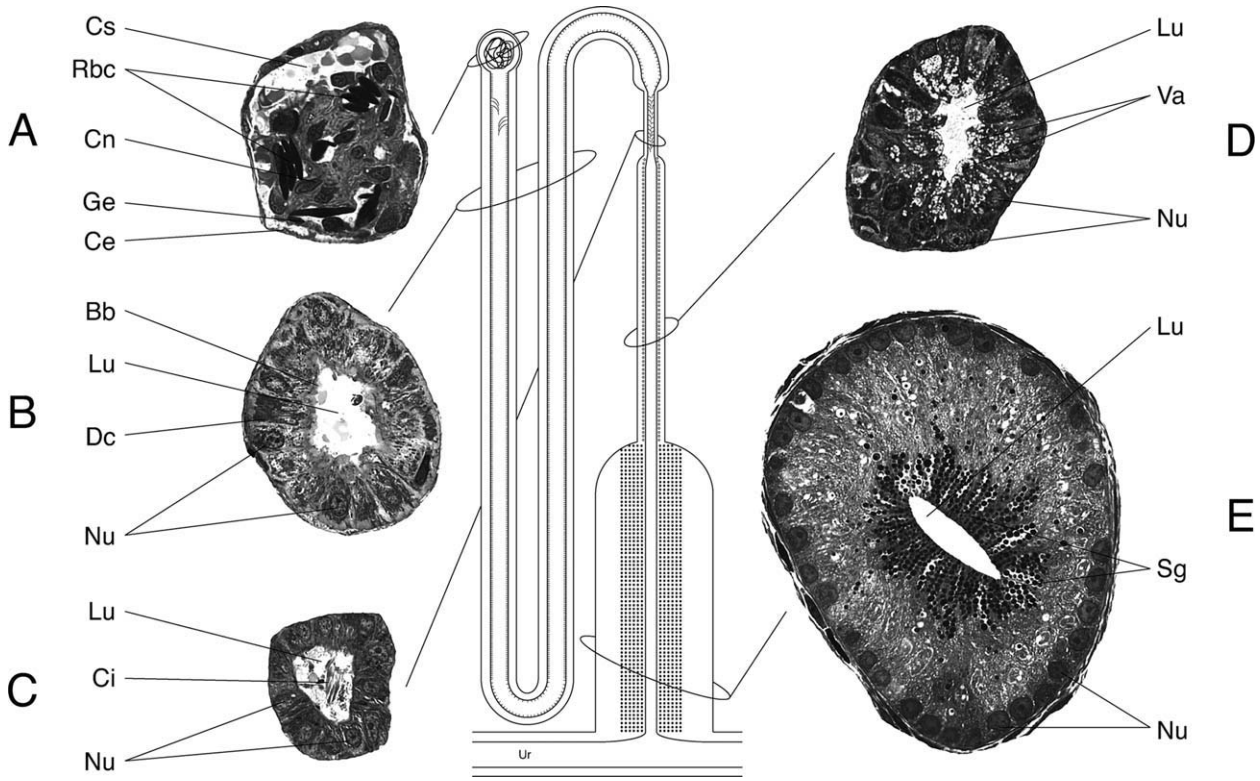

Fig. 2. Schematic drawing of the nephron in *H. turcicus,* constructed from visual estimates of the nephrons regionality, detailing the histology of each region. The bends do not actually represent the coiled morphology of the nephrons (e.g., in histological section, the proximal portion of the distal convoluted tubule lies adjacent to the renal corpuscle). **A.** Renal corpuscle with associated glomerulus. Cs, capsular space; Rbc, red blood cell; Cn, capillary nuclei; Ge, glomerular epithelium; Ce, capsular epithelium. **B.** Proximal convoluted tubule. BB, brush border; Lu, lumen; Dc, dark cell; Nu, nucleus. **C.** Intermediate segment connecting the proximal convoluted tubule and distal convoluted tubule. Lu, lumen; Ci, cilia, Nu, nucleus. **D.** Distal convoluted tubule. Lu, lumen; Va, vacuoles; Nu, nucleus. E. Sexual segment. Lu, lumen; Sg, secretory granule; Nu, nucleus.

plasmic contents and basal nuclei that often posses a centralized nucleolus.

The nonciliated epithelial cells of the proximal convoluted tubule are filled with dark staining cytoplasmic contents (toluidine blue) and basal nuclei (Fig. 2B; Nu) that usually posses a centralized nucleolus (Fig. 2B). The epithelium of the proximal convoluted tubule stains positively with alcian blue (Fig. 3B) and bromphenol blue (Fig. 3C) and contains a low microvillus brush boarder that lines the apices of the epithelial cells (Fig. 2B). Diffuse material is often found in the lumen and associated with the apical regions of the epithelial cells. At the proximal region of this segment ciliated cells with dark cytoplasm are found intermixed with the nonciliated epithelial cells described above.

The intermediate segment (Fig. 2C) unites the proximal and distal convoluted tubules. This segment is lined by a simple cuboidal epithelium with dark staining cytoplasm (toluidine blue). Nuclei are in a basal position and typically possess a centrally located nucleolus. Elongate cilia (Fig. 2C; Ci) form at the apices of all of the epithelial cells in this region and protrude into the lumen with their terminal ends oriented toward the distal regions of the nephron. This region does not stain positive with any histochemical stains used (Fig. 3).

The distal convoluted tubule (Fig. 2D) is lined by a simple columnar epithelium. Like the anterior regions of the proximal convoluted tubule, the proximal region of the distal convoluted tubule possesses sporadically positioned ciliated cells. Intermixed with these ciliated cells in the proximal region of this segment, and the primary cell type in the more distal regions of this segment, are epithelial cells packed with lucent secretory vacuoles (Fig. 2D; Va) at their apices. Nuclei (Fig. 2D; Nu) are located in a basal position and typically possess a centrally located nucleolus. Diffuse secretory material is often found in the lumen of this segment. This region stains positively with alcian blue (Fig. 3B) and bromphenol blue (Fig. 3C). At the distal most extremity of the distal convoluted tubule, the apical vacuoles fill with dark staining granules and the epithelial height increases dramatically, demarcating the transition to the SSK (Fig. 2E).

The sexual segment is lined by a tall columnar epithelium with basally positioned nuclei (Fig. 2E;

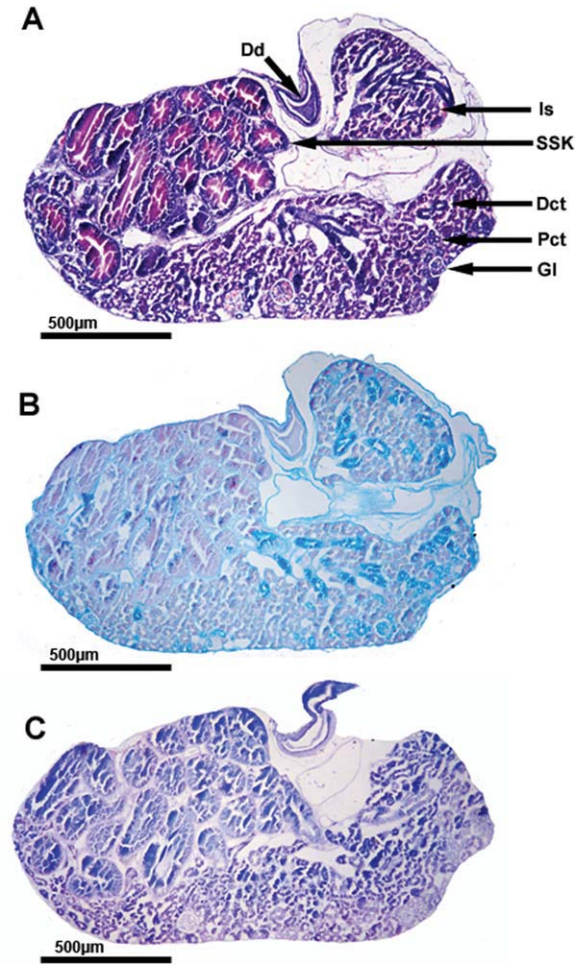

Fig. 3. Histochemical analysis of the kidney in *H. turcicus*. **A.** Hematoxylin and eosin stain showing the general morphology of the cross-sectional area for which histochemical analyses were taken. **B.** Periodic Schiff's stain of the kidney showing the magenta stain of the collecting duct (SSK) and alcian blue positive stain for the proximal convoluted tubules. **C.** Bromphenol blue stain of the kidney detailing the positive reaction to bromphenol blue by the collecting duct (SSK).

Nu), which often contain a centrally located nucleolus (Fig. 2E). Dark secretory granules (Fig. 2E; Sg) fill the apices of all of the epithelial cells in this region. The sexual segment empties into the ureter differentiating the distal extremity of the nephron. The SSK reacts positively with PAS (Fig. 3B) and with bromphenol blue (Fig. 3C).

Figure 4 depicts the activity of the SSK in comparison with other major reproductive events previously investigated in male and female *H. turcicus*. Activity of the SSK begins in March (Fig. 4) with the hypertrophy of the collecting duct. Hypertrophy of the SSK continues through August (Fig. 4) with dense secretory granules within the cytoplasm. By September, the collecting tubule is no longer hypertrophied and does not stain positively with any histochemical stains. During this time, the SSK appears similar to the other regions of the nephron (Fig. 5A, black box). The SSK remains nonhypertrophied until March when activity begins again. A reproductively active female *H. turcicus* also did not possess a hypertrophied SSK (Fig. 5B).

Ultrastructure

The tubules of the SSK are lined with a simple columnar epithelium (Fig. 6A,B; Ep) surrounding a centralized lumen (Fig. 6A,B, Lu). The nuclei (Fig. 7A; Nu) are euchromatic, usually contain a dark staining centralized nucleolus (Fig. 7A; No), and are positioned in close association with the basal lamina (Fig. 7A; Bl). The cytoplasm of the epithelial cells contains perinuclear rough endoplasmic reticulum (Fig. 7C; Rer) and extensive Golgi complexes (Fig. 7C; Gc). Multiple electron-lucent vesicles (Fig. 7C; Gv) can be seen budding from the Golgi complexes. From the Golgi complexes, the Golgi vesicles (Fig. 7C Inset, black arrowhead) can be seen merging to form condensing vacuoles (Fig. 7C Inset, white arrowhead). The condensing vacuoles (Fig. 7B; Cv) migrate apically and become homogenous electron-dense secretory granules (Figs. 6 and 7A,B; Sg) before being released into the lumen by a merocrine style secretion (e.g., vacuole fusion with apical plasma membrane; Fig. 7A; Mr). Small microvilli (Fig. 7B; Mv) extend into the lumen (Fig. 7B; Lu), and the cells are joined at the luminal aspect by tight junctions (Fig. 7B; Tj) sealing the intercellular canaliculi.6

The basal tubular region of the SSK contains the nuclei of the columnar epithelial cells. The intercellular canaliculi (Fig. 8A,B; Ic) are very narrow and nonlabyrinthine, but few junctional complexes occur deep to the apical tight junctions. Monocytic leukocytes (Fig. 8A; Lk) can be seen both inside the basal lamina (Fig. 8A; Bl), within intercellular canaliculi (Fig. 8A; Ic), and exterior to the basal lamina. Capillaries (Fig. 8B; Cp) and

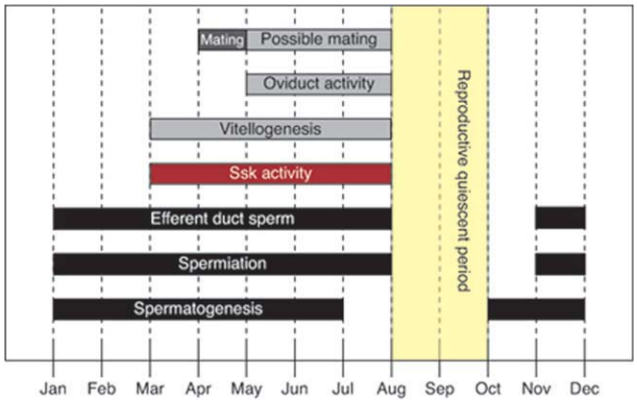

Fig. 4. Graph of reproductive activity in both male and female *H. turcicus*.

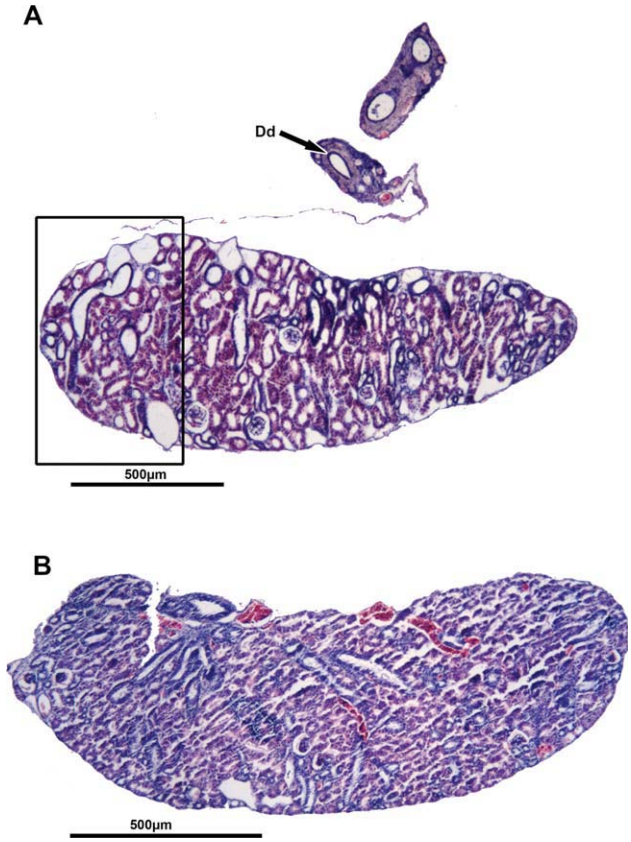

Fig. 5. Inactive states of the kidneys in *H. turcicus*. **A.** Inactive state in the male showing the region of the renal sexual segment (black box) and the position of the ductus deferens (Dd). **B.** Kidney of the female during April showing no hypertrophic regions of the kidney.

mast cells (Fig. 8B; Mc) can both be found outside the basal lamina of the SSK tubules. The mast cells contain large amounts of granulated material as well as some membranous material.

During the inactive months (September–February) the SSK is not discernible from the other regions of the collecting duct (Fig. 5A; outline). During this time, cellular height decreases, and few remnant secretory granules are seen in the apices of the epithelial cells (Fig. 9A,B; Sg). The nucleus is euchromatic with a dark staining centralized nucleolus. No prominent Golgi complexes or rough endoplasmic reticulum are observed. Intercellular canaliculi (Fig. 9A,B; Ic) are straight and narrow as in active cells. Several cytoplasmic spaces are observed in the apical portions of the cell (Fig. 9B; Cs) and basal portions of the cell (Fig. 9C; Cs) near the basal lamina (Fig. 9C; Bl).

Evolution of SSK Location

When mapped onto the morphological phylogeny of Conrad (2008) (Fig. 10A), the ancestral state of both Lepidosauria and Squamata are recovered as equivocal. The SSK involving the distal convoluted tubule, collecting duct, and ureter unites the Iguanomorpha, and convergence is seen in Teiidae and Scolecophidians. The SSK, being limited to the collecting ducts, unites the Gekkonidae, although the ancestral state is rendered as equivocal due to missing data in Pygopodidae. This state is also observed within Xantusiidae and *P. taurica*. Within the Lacertidae, except *P. taurica*, the SSK involves the collecting duct and ureter. This character state is also observed within the Scincomorpha, with the exception of Serpentes and Anguidae. All Alethinophidia are united by the SSK being limited to the distal convoluted tubule. Varanidae is unique with the SSK being limited to the intermediate segment of the nephron.

Using the molecular phylogeny of Eckstut et al. (2009b) (Fig. 10B), the ancestral state of the Lepi-

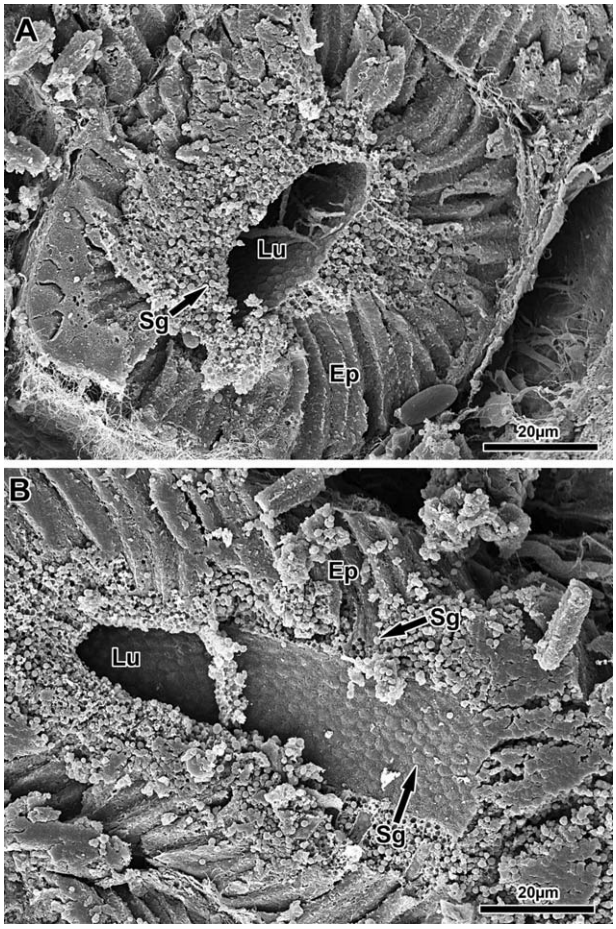

Fig. 6. Scanning electron microscopy of the sexual segment. **A.** Cross section of the renal sexual segment tubule detailing the simple columnar epithelium (Ep), secretory granules (Sg), and lumen (Lu). **B.** Transverse section of the sexual segment tubule detailing secretory granules (Sg) preparing to be released into the lumen (Lu).

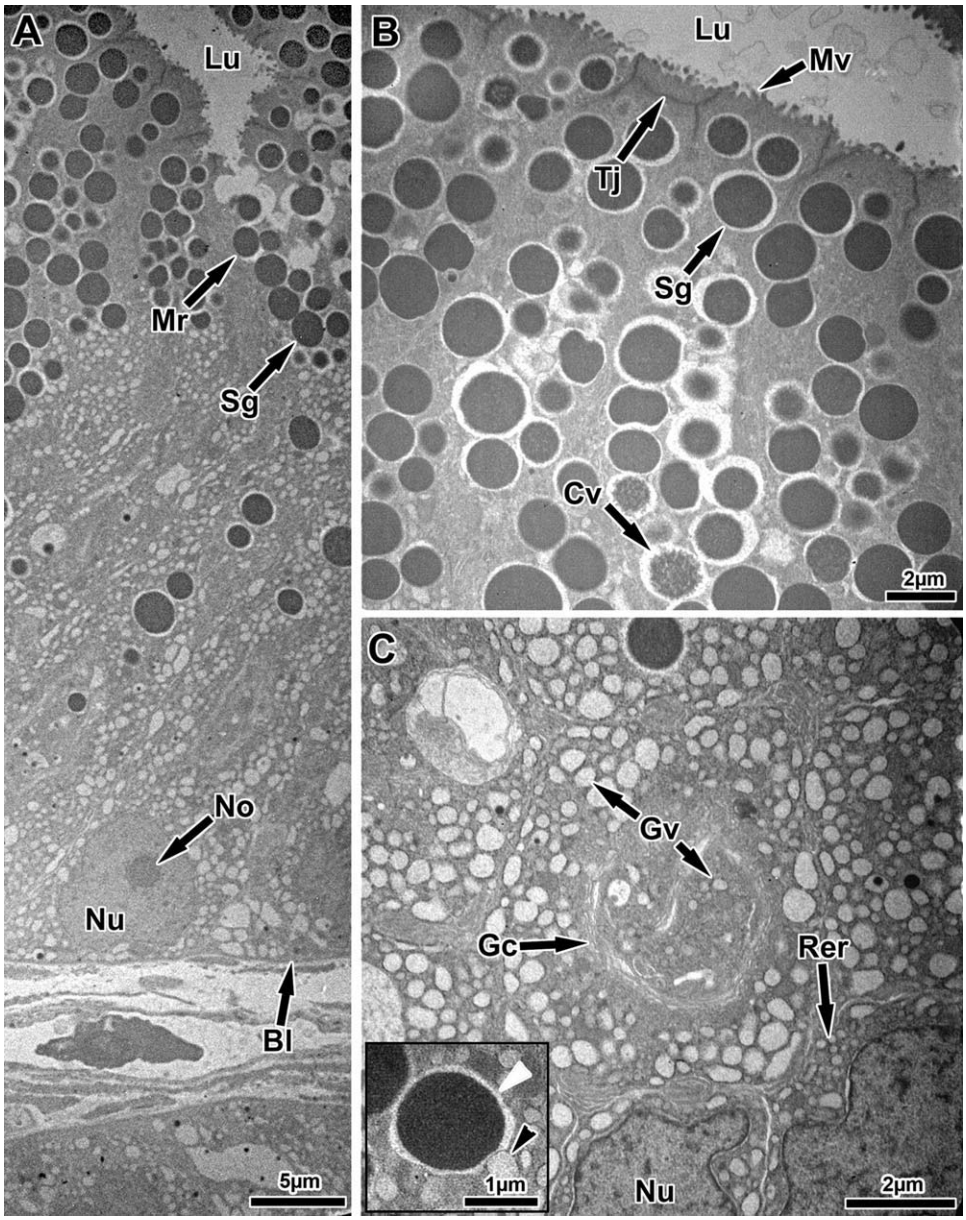

Fig. 7. Transmission electron microscopy of the sexual segment. **A.** Overview of the SSK detailing the large columnar epithelium with basal nuclei (Nu) and central nucleaolus (No). Large secretory granules (Sg) are released into the lumen (Lu) by merocrine secretion (Mr). **B.** Apical portion of an epithelial cell detailing the apical tight junctions (Tj) and microvilli (Mv) extending into the lumen (Lu). Both condensing granules (Cg) and secretory granules (Sg) can be found in the apical portion. **C.** Basal portion of an epithelial cell detailing the nucleus (Nu) and juxtapositioned rough endoplasmic reticulum (Rer). Large Golgi complexes (Gc) are seen apical to the nuclei with multiple Golgi vesicles (Gv). Inset: Golgi vesicle (black arrowhead) merging with a secretory granule (white arrowhead).

dosauria and Squamata are resolved as the SSK including the distal convoluted tubule, collecting ducts, and portions of the ureter. The first character change is within Gekkonidae, which are united with the SSK being limited to the collecting duct, and convergence is observed within *P. taurica*. Within the Scincidae–Rhineuridae clade, the SSK includes the collecting ducts and portions of the ureter with convergence being observed in Anguidae. The Varanidae is unique with the SSK being limited to the intermediate segment. The derived snakes are united with the SSK being limited to the distal convoluted tubule and the paraphyletic status of the Scolecophidia render the ancestral character being the SSK including the collecting ducts and portions of the ureter, which is seen in all other squamates investigated.

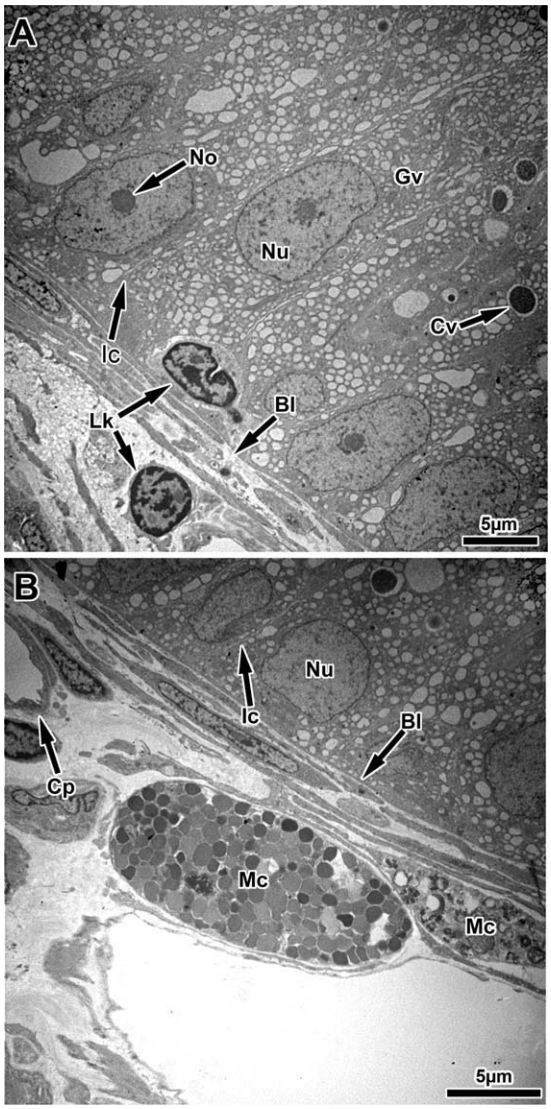

Fig. 8. Transmission electron microscopy of the SSK. **A.** Basal portion of the epithelium detailing the nucleus (Nu) with a central nucleolus (No). Leukocytes (Lk) can be found both within and outside of the basal lamina (Bl). Golgi vesicles (Gv) and cytoplasmic vesicles (Cv) are also observed. **B.** Basal view of the epithelium detailing the basal nucleus (Nu) and secretory granule (Sg). A large mast cell (Mc) sets outside the basal lamina (Bl) within the extracellular matrix (Ecm).

DISCUSSION

Since the first description of the SSK by Gampert (1866), numerous studies have been conducted detailing the morphology of the SSK in squamates. The nephron structure is similar to what has been described in most squamates with the SSK being limited to the distal portions of the uriniferous tubules (Anderson, 1960; Misra et al., 1965; Sever et al., 2002; Krohmer, 2004; Siegel et al., 2009). Inconsistencies observed in the exact location of the SSK within squamates have confounded the terminology used in keeping synonymous nomenclature between lizards and snakes. Within snakes, the SSK appears to be limited to the distal convoluted tubules, and up to three different regions of the distal convoluted tubule have been recognized (Regaud and Policard, 1903; Fox, 1952; Sever et al., 2002; Krohmer, 2004; Sever and Hopkins, 2005; Siegel et al., 2009). The preterminal segment is limited to the anterior region of the distal convoluted tubule (Fox, 1952), the terminal segment is the body of the distal convoluted tubule (Fox, 1977), and the postterminal segment is limited to the most posterior portion of the distal convoluted tubule before entering the collecting duct (Gabe, 1959). However, within the Scolecophida, Fox (1965) described the SSK being limited to the collecting duct and anterior portion of the ureter.

Within lizards, the SSK shows some variation in its location. In the Gekkonidae including *H. turcicus*, the SSK is limited to the collecting duct. Within the Teiidae, Gymnopthalmidae, Agamidae, Chamaeleonidae, and Iguanidae, the SSK resembles that of the Scolecophidia in which it includes the collecting duct and at least some portions of the ureter. *Varanus* is unique with the SSK limited to the intermediate segment of the nephron (Saint Girons, 1972). In all other squamates investigated to date, the SSK includes the distal convoluted tubule, collecting ducts, and portions of the ureter.

Evolution of the SSK location shows variation between the two phylogenies utilized as a result of their respective hypothesized internal relationships. Using the C-mos tree proposed by Eckstut et al. (2009b), the ancestral condition of the Lepidosauria is resolved as the SSK includes the distal convoluted tubule, collecting duct and portions of the ureter. However, Gabe and Saint Girons (1964) hypothesize that only the distal piece of the intermediate segment may become hypertrophied during the active season in *Sphenodon*, which is similar to *Varanus*. All of the Alethinophidia are united by the SSK being limited to the distal convoluted tubule. The topology proposed by Conrad (2008) recovers the relationship between the Scolecophidia and Alethinophidia unresolved where the Eckstut et al. (2009b) phylogeny renders the Scolecophidia paraphyletic. This changes the ancestral character state from being equivocal to the SSK including the collecting duct and portions of the ureter unequivocally the ancestral state for snakes. Interesting to note is the difference of *P. taurica* within Lacertidae. The study on *P. taurica* stated the SSK was limited to the collecting duct but no mention of the ureter was made, leading to the possibility that involvement of the ureter in the SSK of *P. taurica* was overlooked. It is premature to discuss the evolution of reproductive morphological characters based on the number of taxa that are currently unrepresented for SSK morphology.

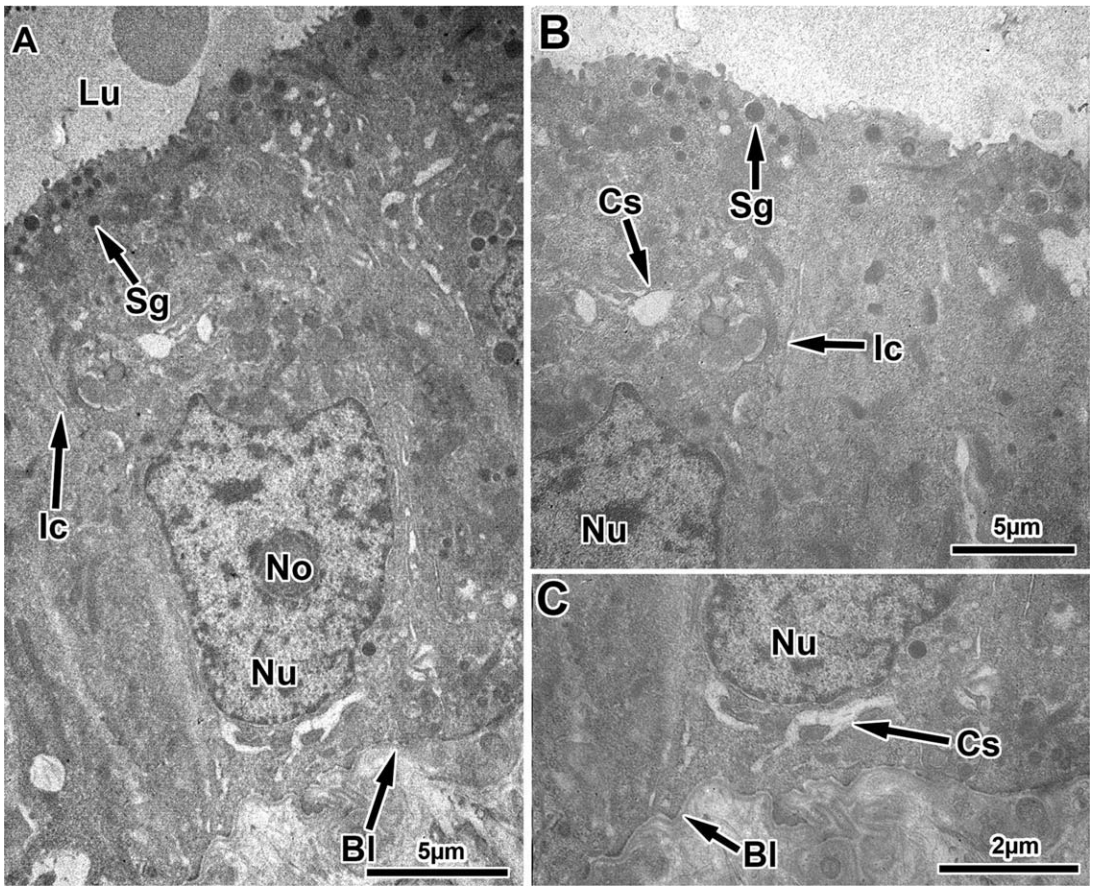

Fig. 9. Transmission electron microscopy of the inactive sexual segment. **A.** Overview of an epithelial cell showing the tall columnar epithelium with the lumen (Lu), reduced number of secretory granules (Sg), intercellular canaliculi (Ic), nucleus (Nu), nucleolus (No), and basal lamina (Bl). **B.** Apical portion of an epithelial cell detailing the secretory granules (Sg), cytoplasmic spaces (Cs), intercellular canaliculi (Ic), and nucleus (Nu). **C.** Basal portion of an epithelial cell detailing the nucleus (Nu), cytoplasmic spaces (Cs), and basal lamina (Bl).

The seasonal variation within the SSK of *H. turcicus* parallels the data presented by Rheubert et al. (2009) on spermatogenic activity, and the variation within the testicular ducts (Rheubert et al., 2010). Activity begins in March and continues through August (Fig. 4). These data on SSK activity strongly correlate with data on sperm presence within the testicular ducts of males and vitellogenesis in females. During the times when copious amounts of sperm are present within the testicular ducts (Rheubert et al., 2010), the SSK is hypertrophied. Johnson (1982) reported that SSK activity mirrored data from androgen levels in the cottonmouth snake *Agkistrodon piscivorus* but, interestingly, the SSK in *H. turcicus* continues activity even after spermatogenesis has entered a quiescent period (presumably when androgen levels decrease) while sperm are still present in the efferent ducts. The activity of the SSK is also highly correlated with the proposed mating season and female vitellogenesis and oviductal cycle in the Mediterranean Gecko (Fig. 4; Eckstut et al., 2009a), a condition similar to that described for the snake *A. piscivorus*. Seasonal fluctuations in SSK activity, efferent duct activity, and spermatogenesis are significant in an analysis of overall reproductive energy costs for male *H. turcicus*. Schaffer (1974), Bull and Shine (1979), and Olsson et al. (1997) noted that periods of nonlinearities between reproductive costs and benefits vary with optimal life history strategies based on periods of increased reproductive energy allocation.

Inactive SSK tubules of *H. turcicus* undergo complete regression, which has also been reported in some other lizards (Sanyal and Prasad, 1966; Fox, 1977; Gabri, 1983). In some snakes secretory activity is only reduced, and the SSK is still distinguishable from other portions of the nephron throughout the year (Sever et al., 2002; Krohmer, 2004; Sever et al., 2008). Although Prasad and Sanyal (1969) found no stimulatory effects on the SSK with estrogen and progesterone, they found that anabolic and androgenic steroids stimulate SSK development, and Billy and Crews (1986) corroborated their data. Most temperate snakes exhibit a postnuptial spermatogenic pattern and

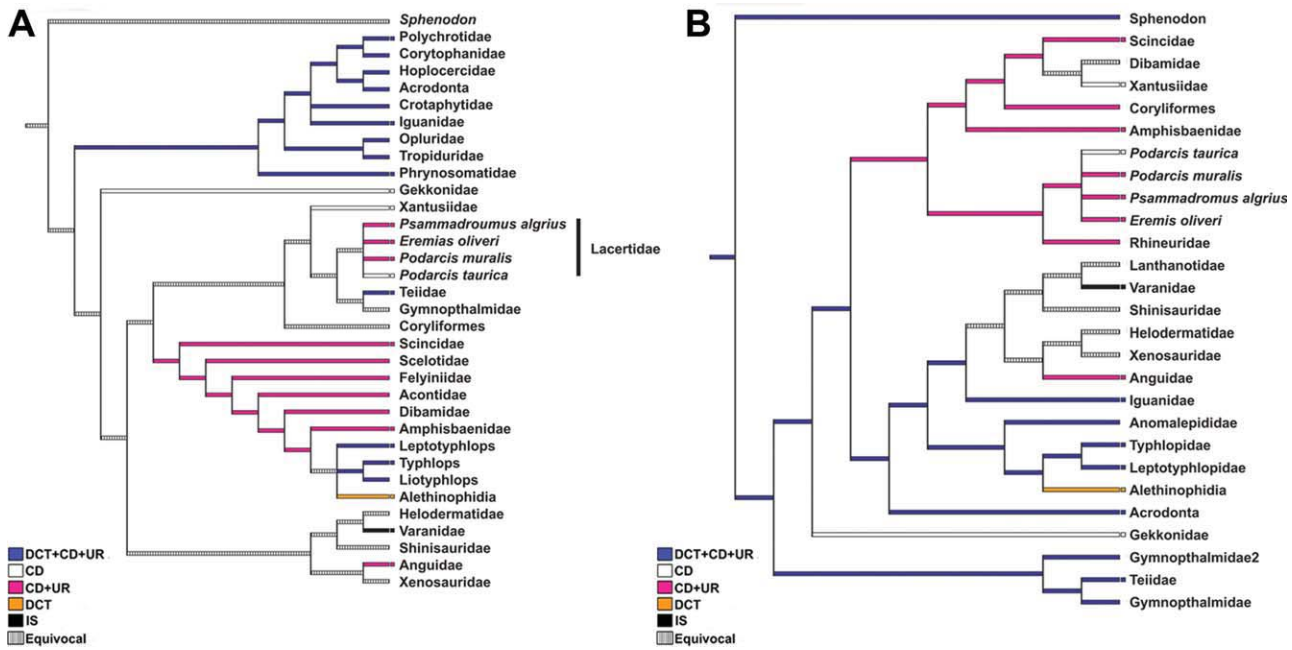

Fig. 10. Parsimony optimization of SSK location onto the **A.** Morphological tree adapted from Conrad (2008) and **B.** Molecular tree adapted from Eckstut et al. (2009b).

store sperm in the ductus deferens throughout the year until mating (S. Goldberg, personal communication). With the postnuptial spermatogenic cycle, androgen levels may remain increased throughout the year and thus may lead to a continuously hypertrophied SSK. However, most temperate lizards exhibit a prenuptial spermatogenic cycle (R. Aldridge, personal communication), and sperm are evacuated from the efferent ducts during mating. This may lead to a dramatic decrease in androgen levels during the reproductively inactive season which may result in the SSK becoming regressed.

Most of the ultrastructural descriptions of the SSK describe a tall columnar epithelium (Table 1). The natricine snakes and some old world vipers exhibit and epithelium containing centrally located nuclei (Sever et al., 2002; Siegel et al., 2009), whereas all others have basally positioned nuclei (Sever and Hopkins, 2005; Sever et al., 2008) similar to *H. turcicus*. Large electron dense secretory granules that stain positively for carbohydrates (PAS) and proteins (bromphenol blue) during the active season are observed in *H. turcicus*. Saint Girons (1972) found that the secretory granules in the 73 species of 19 families he studied were always rich in protein, but the PAS reaction was quite variable, and histochemical studies since then (Table 1) have corroborated his data. Both *C. lemniscatus* (Del Conte, 1972) and *A. piscivorus* (Sever et al., 2008) contain cells with secretory granules of various sizes within the apical cytoplasm. Some lizards including *S. lateralis* contain cells with secretory granules that have an electron-lucent collar surrounding them that was not observed in *H. turcicus*. However, all other studies show results similar to *H. turcicus* in which the secretory granules are similar in size and homogenous in electron density. These granules are released by a merocrine secretion as predicted in the northern watersnake, *Nerodia sipedon* (Krohmer, 2004), and observed in the electron-lucent granules of *A. piscivorus* (Sever et al., 2008), whereas the SSK epithelium in black swamp snakes, S*eminatrix pygaea* (Sever et al., 2002), brown treesnakes, *Boiga irregularis* (Siegel et al., 2009), and *P. taurica* (Gabri, 1983) release secretory granules in an apocrine manner (Table 1).

All studies regarding the ultrastructure of the SSK report extensive Golgi complexes as observed in *H. turcicus*. The Golgi complex of *H. turcicus* is arranged concentrically like the Golgi complexes of *A. piscivorus* (Sever et al., 2008), S*cincella lateraialis* (Sever and Hopkins, 2005), and *B. irregularis* (Siegel et al., 2009; Table 1). The presence of rough endoplasmic reticulum occurs in the SSK of *H. turcicus* but is often obscured by Golgi vesicles and condensing vacuoles. The intercellular canaliculi of *H. turcicus* are narrow and nonlabyrinthine similar to *B. irregularis* (Siegel et al., 2009), which differs from reports in the snake *A. piscivorus* (Sever et al., 2008) and the lizards *C. lemniscatus* (Del Conte, 1972) and *P. taurica* (Gabri, 1983). The intercellular canaliculi in these species also remain wide even during the inactive season. In *H. turcicus*, the intercellular canaliculi are very narrow

TABLE 1. Table of ultrastructural studies on squamate SSK with various cellular characteristics

	A. piscivorus	*N. natrix*	*S. pygaea*	*C. lemniscatus*	*N. sipedon*	*L. sicula*	*P. taurica*	*S. lateralis*	*B. irregularis*	*H. turcicus*
Epithelium	Columnar	Columnar	Columnar	Columnar	Columnar	Columnar	Columnar	Columnar	Columnar	Columnar
Nuclei	Basal	Basal	Central	Basal	Basal	Basal	Basal	Basal	Central	Basal
Secretion mode	Merocrine/ apocrine	Apocrine	Apocrine	Merocrine	N/a	N/a	N/a	Apocrine	Atypical apocrine	Merocrine
Secretory granules	Electron dense	Electron dense	Electron dense	Electron dense	Electron dense	Electron dense	Electron dense	Electron dense	Electron dense	Electron dense
PAS+	Yes	No	Yes	Yes	N/a	N/a	N/a	Yes	Yes	Yes
BB+	Yes	Yes	Yes	N/a	N/a	N/a	N/a	Yes	Yes	Yes
Golgi complex	Concentric	Linear	Linear	Linear	N/a	Linear	Linear	Linear/ concentric	Concentric	Concentric
Rer	Elaborate	Not elaborate	Elaborate	Elaborate	Elaborate	Elaborate	Elaborate	Elaborate	Elaborate	Elaborate
Occurrence in female	Absent	Not studied	Not studied	Similar but less developed	Not studied	Not studied	Absent	Similar but less developed	Not studied	Absent
Source	Sever et al., 2008	Kühnel and Krisch, 1974	Sever et al., 2002	Del Conte and Tamayo, 1973	Krohmer, 2004	Furieri and Lanzavecchiea, 1959	Gabri, 1983	Sever and Hopkins, 2005	Siegel et al., 2009	This study

during both the active and inactive season similar to *S. lateralis* (Sever and Hopkins, 2005).

During the inactive season, SSK tubules of *H. turcicus* consists of low columnar epithelial cells with few remnant secretory granules and no prominent Golgi complexes or rough endoplasmic reticulum. Previous reports on the inactive SSK, in lizards, suggest the epithelium is cuboidal with basal nuclei (Gabri, 1983; Sever and Hopkins, 2005). These reports all show prominent Golgi complexes and in *P. taurica* a distended rough endoplasmic reticulum with mucoidal vacuoles. The appearance of cells in squamates in which seasonal regression of the SSK occurs may vary greatly based on the portion of the nephron that comprises the SSK.

In the lizards, *S. lateralis* (Sever and Hopkins, 2005) and *C. lemniscatus* (Del Conte, 1972) females show a hypertrophied SSK similar to that in males. However, in *H. turcicus*, like the Balkan wall lizard, *P. taurica*, and the yellowbellied house gecko, *H. flaviviridis*, hypertrophy does not occur in the nephrons examined from a reproductively active female.

The SSK in squamates has been considered an important part of the reproductive biology in squamates (Sever and Hopkins, 2005), and knowledge of its variation is essential for fully understanding reproductive cycles of lizards and snakes. With increasing data on reproductive characteristics within reptiles (germ cell development, efferent duct morphology, sperm storage cycles, cloacal morphology, and SSK morphology), better analyses of reproductive cycles and phylogenetic analyses can be performed. Furthermore, morphological work on male reproductive systems in squamates is needed to investigate a wider range of this taxonomically, morphologically, and ecologically diverse group of vertebrates.

ACKNOWLEDGMENTS

The authors would like to thank Dr. Brian Crother, Dr. Kevin Gribbins, and Dr. Kyle Piller for their useful comments on an earlier draft of this manuscript and also Mallory Eckstut and Ryan Chabarria for their help in collection of specimens.

LITERATURE CITED

Aldridge RD, Siegel DS, Jellen B. The sexual segment of the kidney. In: Aldridge RD, Sever,DM editors. Reproductive Biology and Phylogeny of Snakes. Enfield, New Hampshire: Science Publishers Inc. (in press).

Anderson E. 1960. The ultramicroscopic structure of a reptilian kidney. J Morphol 106:205–241.

Billy AJ, Crews D. 1986. The effects of sex steroid treatments on sexual differentiation in a unisexual lizard, *Cnemidophorus uniparens* (Teiidae). J Morphol 187:129–142.

Bishop JE. 1959. A histological and histochemical study of the kidney tubules of the common garter snake, *Thamnophis sirtalis*, with special reference to the sexual segment in the male. J Morphol 104:307–357.

Bull JJ, Shine R. 1979. Iteroparous animals that skip opportunities for reproduction. Am Nat 114:296–316.

Conrad JL. 2008. Phylogeny and systematics of squamata (Reptilia) based on morphology. Bull Am Mus Nat Hist 310:1–182.

Courrier R. 1922. Etude préliminaire du déterminisme des caractères sexuels secondaires chez les poisons. Archives d'Anatomie d'Histologie et d'Embryologie Experimentale. 1:115–144.

Cuellar O. 1966. Ociducal anatomy and sperm storage structures in lizards. J Morphol 119:7–20.

Del Conte E. 1972. Granular secretion in the kidney sexual segments of female lizards, *Cnemidophorus l. lemniscatus* (Sauria, Teiidae). J Morphol 137:181–192.

Del Conte E, Tamayo JG. 1973. Ultrastructure of the sexual segments of the kidneys in male and female lizards, *Cnemidophorus l. lemniscatus* (L.). Z Zellforsch Mikrosk Anat 144:325–327.

Devine MC. 1975. Copulatory plugs: Enforced chastity. Science 187:844–845.

Eckstut ME, Lemons ER, Sever DM. 2009a. Annual dynamics of sperm production and storage in the Mediterranean Gecko, *Hemidactylus turcicus*, in the southeastern United States. Amphibia-Reptilia 30:45–56.

Eckstut ME, Sever DM, White ME, Crother BI. 2009b. Phylogenetic analysis of sperm storage in female squamates. In: Dahnof LT, editor. Animal Reproduction: New Research Developments. Happauge, New York: NOVA Science Publishers Inc. pp 185–218.

Fox W. 1952. Seasonal variation in the male reproductive system of Pacific coast garter snakes. J Morphol 91:481–553.

Fox W. 1965. A comparison of the male urogenital systems of blind snakes, Leptotyphlopidae and Typhlopidae. Herpetologica 21:241–256.

Fox H. 1977. The urinogenital system of reptiles. In: Gans C, Parsons TS, editors Biology of the Reptilia, Vol. 6., Morphology E. New York: Academic Press. pp 1–157.

Furieri P, Lanzavecchiea G. 1959. Le secrezione dell; epididimo e del rene sessuale nei rettili. Studio al microscopio elettronico. Arch Ital Anat Embriol 64:357–379.

Gabe M. 1959. Donnees histochimiques sur le rein de *Vipera aspis*. Ann histochim 4:23–31.

Gabe M, Saint Girons H. 1964. Contribution a l'histologie de *Sphenodon punctatus* Gray. Paris: Editions du Centre National de la Recherche Scientifique.

Gabri MS. 1983. Seasonal changes in the ultrastructure of the kidney collecting tubule in the lizard *Podarcis* (=*Lacerta*) *taurica*. J Morphol 175:143–151.

Gampert O. 1866. Ueber die Niere von *Tropidonotus natrix* und der Cyprinoiden. Zeit Wissen Zool 16:369–373.

Johnson LF, Jacob JS, Torrance P. 1982. Annual testicular and androgenic cycles of the Cottonmouth (*Agkistrodon piscivorus*) in Alabama. Herpetologica 38:16–25

Krohmer RW. 1986. Effects of mammalian gonadotropins (oFSH and oLH) on testicular development in the immature water snake, *Nerodia sipedon*. Gen Comp Endocrinol 64: 330–338.

Krohmer RW. 2004. Variation in seasonal ultrastructure of sexual granules in the renal sexual segment of the Northern Water Snake, *Nerodia sipedon sipedon*. J Morphol 261:70–80.

Kuhmel W, Krisch B. 1974. On the sexual segment of the kidney in the snake (*Natrix natrix*). Cell Tissue Res 148:412–429.

Maddison D, Maddison WP. 2005. MacClade Version 4.08. Sunderland, MA: Sinauer Associates, Inc.

Misra UK, Sanyal MK, Prasad MRN. 1965. Phospholipids of the sexual segment of the kidney of the Indian House Lizard, *Hemidactylus flaviviridis* Ruppell. Life Sci 4:159–166.

Olsson M, Madsen T, Shine R. 1997. Is sperm really so cheap? Costs of reproduction in male adders, *Vipera berus*. Proc Royal Soc Biol 264:455–459.

Pandha SK, Thapliyal JP. 1964. Effect of male hormone on the renal segment of the castrated male of the lizard *Calotes versicolor*. Copeia 1964:579–581.

Prasad MRN, Reddy PRK. 1972. Physiology of the sexual segment of the kidney in reptiles. Gen Comp Endocrinol (Suppl 3):649–662.

Prasad MRN, Sanyal MK. 1969. Effect of sex hormone on the sexual segment of the kidney and other accessory reproductive organs of the Indian House Lizard *Hemidactylus flaviviridis* Ruppell. Gen Comp Endocrinol 12:110–118.

Regaud C, Policard A. 1903. Recherches sur la structure du rein de queques ophidiens. Arch Anat Microsc 6:191–282.

Rheubert JL, Poldemann EH, Eckstut ME, Collier MH, Sever DM, Gribbins KM. 2009. Temporal germ cell development strategy during mixed spermatogenesis within the male Mediterranean Gecko, *Hemidactylus turcicus* (Reptilia: Gekkonidae). Copeia 4:793–800.

Rheubert JL, Sever DM, Geheber AD, Siegel DS. 2010. Proximal testicular ducts of the Mediterranean Gecko (*Hemidactylus turcicus*). Anat Rec 293:2176–2192.

Saint Girons H. 1972. Morphologie compare du segment sexuel du rein des squamates (Reptilia). Arch Anat Microsc Morphol Exp 61:243–266.

Sanyal MK, Prasad MRN. 1966. Sexual segment of the kidney of the Indian House Lizard, *Hemidactylus flaviviridis* Ruppell. J Morphol 118:511–528.

Schaffer WM. 1974. Optimal reproductive efforts in fluctuating environments. Am Nat 964:783–900.

Sever DM, Hopkins WA. 2005. Renal sexual segment of the Ground Skink, *Scincella laterale* (Reptilia, Squamata, Scincidae). J Morphol 266:46–59.

Sever DM, Stevens RA, Ryan TJ, Hamlett WC. 2002. Ultrastructure of the reproductive system of the Black Swamp Snake (*Seminatrix pygaea*). III. Sexual segment of the male kidney. J Morphol 252:238–254.

Sever DM, Siegel DS, Bagwill A, Eckstut ME, Alexander L, Camus A, Morgan C. 2008 Renal sexual segment of the Cottonmouth Snake, *Agkistrodon piscivorus* (Reptilia, Squamata, Viperidae). J Morphol 269:640–653.

Siegel DS, Aldridge RD, Clark CS, Poldemann EH, Gribbins KM. 2009. Stress and reproduction in *Boiga irregularis* with notes on the ultrastructure of the sexual segment of the kidney in squamates. Can J Zool 87:1138–1149.

Siegel DS, Sever DM, Aldridge RD. 2010. The pelvic kidney of male *Ambystoma maculatum* (Amphibia, Urodela, Ambystomatidae) with special reference to the sexual collecting ducts. J Morphol 271:1422–1439.

Volsøe H. 1944. Structure and seasonal variation of the male reproductive organs of *Vipera berus* (L.) København: Spolia Zoologica Musei Hauniensis V. Skrigter, Univeritetets Zoologiske Museum.